

PAPER • OPEN ACCESS

## Aligned magnetic field effect on unsteady liquid film flow of Casson fluid over a stretching surface

To cite this article: M Sailaja *et al* 2017 *IOP Conf. Ser.: Mater. Sci. Eng.* **263** 062008

View the [article online](#) for updates and enhancements.

### Related content

- [Aligned magnetic field of two-phase mixed convection flow in dusty Casson fluid over a stretching sheet with Newtonian heating](#)  
N S Arifin, S M Zokri, A R M Kasim *et al.*
- [Slip Effects On MHD Three Dimensional Flow Of Casson Fluid Over An Exponentially Stretching Surface](#)  
B Madhusudhana Rao, M Krishna Murthy, N Sivakumar *et al.*
- [Diffusive effects on hydrodynamic Casson nanofluid boundary layer flow over a stretching surface](#)  
M I Anwar, N Tanveer, M Z Salleh *et al.*



**ECS** **240th ECS Meeting**  
Oct 10-14, 2021, Orlando, Florida

**Register early and save up to 20% on registration costs**

Early registration deadline Sep 13

**REGISTER NOW**

# Aligned magnetic field effect on unsteady liquid film flow of Casson fluid over a stretching surface

M Sailaja<sup>1</sup>, R Hemadri Reddy<sup>2</sup>, R Saravana<sup>3</sup> and K Avinash<sup>4</sup>

<sup>1</sup> Department of Mathematics, Dravidian University, Kuppam 517 425, India

<sup>2</sup> Department of Mathematics, School of Advanced Science, VIT University, Vellore 632 014, India

<sup>3</sup> Department of Mathematics, Madanapalle Institute of Technology and Science, Madanapalle 517 325, India

<sup>4</sup> Department of Mathematics, Sreyas Institute of Engineering and Technology, Hyderabad 500 068, India

E-mail address: rhreddy@vit.ac.in

**Abstract.** The heat and mass transfer in non-Newtonian fluids plays a major role in technology and in nature due to its stress relaxation, shear thinning and thickening properties. In this study, we investigated the heat and mass transfer in unsteady liquid film flow of Casson fluid in the presence of aligned magnetic field, thermophoresis and Brownian moment effects. The transformed governing boundary layer equations are solved numerically by employing shooting technique. Dual solutions are explored for Newtonian and non-Newtonian cases. The impact of pertinent parameters on the flow, thermal and concentration fields are discussed with the assistance of graphical illustrations. The reduced Nusselt number is reported and discussed through tabular results.

## 1. Introduction

Many researchers have enticed by the concept of heat and mass transfer as they have enormous applications in multiple disciplines such as taxonomy of moisture and temperature amidst, orchard of fruit trees and farming fields. It is well known that when heat and mass transfer occur simultaneously, complex conduct was noticed in the connections between the fluxes and the guiding potentials. It is also observed that the energy flux can be embellished by both concentration and temperature gradients.

Sulochana and Sandeep [1] discussed the dual solution of temperature and mass transfer in a nanofluid over horizontal and exponentially stretching/shrinking cylinders in the presence of shape of nanoparticles, viscous dissipation, suction/injection. By considering two different geometries, Sandeep and Gnaneswara Reddy [2] investigated the heat transfer in Cu-water nanofluid. Crane [3] investigated the closed form of exponential solution of two dimensional flow over a stretching plane. MHD flow past a stretching porous surface has been studied by Pop and Na [4]. Heat and mass transfer of MHD flow over a stretching sheet has been reported sbly Liu [5]. Chiam [6] illustrated the MHD flow past a stretching surface in the presence of power law velocity. Later on, a note on MHD flow over a stretching sheet by taking an account of power-law fluid has been studied by Cortell [7]. Yi-wu [8] investigated the 1-D non-uniform flow. The steady nonlinear MHD flow and heat transfer past a stretching surface of variable temperature have been studied by Anjali Devi and Thiyagarajan [9]. MHD non-Darcy flow and energy transfer past a stretching sheet in presence of Ohmic dissipation and



thermal radiation has been studied by Dulal Pal and Hiranmoy Mondal [10]. Anuar Ishak [11] investigated the MHD boundary layer flow past an exponentially stretching sheet with radiation effect.

Nadeem et al. [12] analysed the homotopy perturbation solution for 2-D Williamson fluid model past a stretching sheet. They found that the non-dimensional velocity  $f'$  decreases and coefficient of skin friction decreases parabolically with increasing the Williamson parameter. Zehra et al. [13] examined the pressure dependent viscosity for Williamson fluid and detected the solution numerically by Runge-Kutta Fehlberg method. Vajravelu et al. [14] investigated the peristaltic pumping of a Casson fluid in contact with a Newtonian fluid with a permeable wall. Vajravelu et al. [15] reported the MHD peristaltic transport of a Carreau fluid under the influence of velocity slip, thermal and concentration jump conditions. Very recently, the researchers [16-22] investigated the heat transfer nature of the MHD flows over various flow geometries.

In this study, we investigated the thermal and mass transfer in unsteady liquid film flow of Casson fluid in the presence of aligned magnetic field, thermophoresis and Brownian moment effects. The transformed governing boundary layer equations are solved numerically by employing shooting technique. Dual solutions are explored for Newtonian and non-Newtonian cases. The impact of pertinent parameters on the flow, thermal and concentration fields are discussed with the assistance of graphical illustrations. The reduced Nusselt number is reported and discussed through tabular results.

## 2. Mathematical formulation

We considered an unsteady 2D film flow of a Casson fluid over a stretched sheet placed along the  $x$ -axis with velocity  $u_w(x,t) = bx/(1-\alpha t)$ , where  $b, \alpha$  constants and the  $y$ -axis is normal to it. It is assumed that the  $T_0$  and  $T_r$  are the slit and reference temperatures and  $C_0$  and  $C_r$  are the slit and reference concentration. An inclined magnetic field is applied along the flow direction as displayed in figure 1.

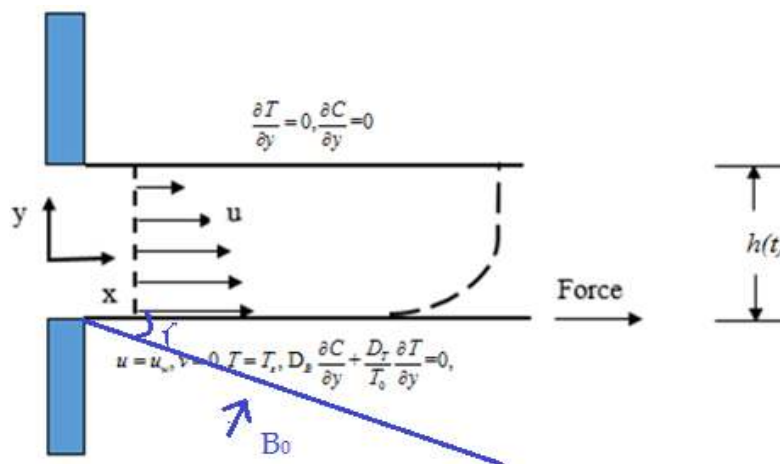


**Figure 1.** Schematic representation

The study is carried out by neglecting induced magnetic field. As per the assumptions above, the unsteady state governing equations in terms of the similarity variable  $\xi$  is defined by  $u = \partial \xi / \partial y$  and  $v = -\partial \xi / \partial x$  are expressed as:

$$\frac{\partial^2 \xi}{\partial x \partial y} - \frac{\partial^2 \xi}{\partial y \partial x} = 0, \quad (1)$$

$$\rho \left( \frac{\partial^2 \xi}{\partial t \partial y} - \frac{\partial^2 \xi}{\partial y^2} \frac{\partial \xi}{\partial x} + \frac{\partial \xi}{\partial y} \frac{\partial^2 \xi}{\partial x \partial y} \right) = \mu \left( 1 + \frac{1}{\delta} \right) \frac{\partial^3 \xi}{\partial y^3} - \sigma \frac{\partial \xi}{\partial y} \sin^2 \gamma B^2(t), \quad (2)$$

$$(\rho c_p) \left( \frac{\partial T}{\partial t} - \frac{\partial T}{\partial y} \frac{\partial \xi}{\partial x} + \frac{\partial T}{\partial x} \frac{\partial \xi}{\partial y} \right) = k \frac{\partial^2 T}{\partial y^2} + (\rho c_p)_s \left( D_B \frac{\partial C}{\partial y} \frac{\partial T}{\partial y} + \frac{D_T}{T_0} \left( \frac{\partial T}{\partial y} \right)^2 \right), \quad (3)$$

$$\left( \frac{\partial C}{\partial t} + \frac{\partial \xi}{\partial y} \frac{\partial C}{\partial x} - \frac{\partial \xi}{\partial x} \frac{\partial C}{\partial y} \right) = D_B \frac{\partial^2 C}{\partial y^2} + \frac{D_T}{T_0} \frac{\partial^2 T}{\partial y^2}, \quad (4)$$

with the conditions

$$\left. \begin{aligned} u = u_w, v = 0, T = T_s, D_B \frac{\partial C}{\partial y} + \frac{D_T}{T_0} \frac{\partial T}{\partial y} = 0, \text{ at } y = 0 \\ \frac{\partial u}{\partial y} = 0, \frac{\partial T}{\partial y} = 0, \frac{\partial C}{\partial y} = 0 \text{ at } y = h, v = \frac{dh}{dt} \text{ as } y = h(t) \end{aligned} \right\} \quad (5)$$

where  $\xi$  represents the stream function,  $u$  and  $v$  are the velocity components,  $\rho$  represents the density,  $\delta$  denotes Casson fluid parameter,  $\mu$  indicates dynamic viscosity,  $\sigma$  indicates the electrical conductivity,  $B(t)$  is the applied uniform magnetic field,  $T$  and  $C$  are the thermal and concentration,  $(\rho c_p)$  represent the specific heat capacitance,  $k$  denotes thermal conductivity of the nanofluid,  $D_T$  and  $D_B$  are the thermophoresis and Brownian diffusion coefficients.

To get an inside analysis of the problem, we use the following similarity transformation.

$$\begin{aligned} \zeta = \left( \frac{b}{v_f(1-\alpha t)} \right)^{0.5} y, \xi = \beta \left( \frac{v_f b}{(1-\alpha t)} \right)^{0.5} x f(\eta), \\ T = T_0 + T_r (bx^2 / 2v_f)(1-\alpha t)^{-1.5} \theta(\eta), B(t) = B_0(1-\alpha t)^{-0.5} \\ C = C_0 + C_r (bx^2 / 2v_f)(1-\alpha t)^{-1.5} \chi(\eta), \end{aligned} \quad (6)$$

where  $\zeta$  is the similarity variable,  $\beta > 0$  is the dimensionless film thickness.  $f, \theta$  and  $\chi$  are dimensionless flow, thermal and concentration fields.

By making use of Eq. (5), the Eqs. (1) to (4) can be transformed as

$$\left( 1 + \frac{1}{\delta} \right) \frac{\partial^3 f}{\partial \zeta^3} + \lambda \left( \frac{\partial^2 f}{\partial \zeta^2} f - \left( \frac{\partial f}{\partial \zeta} \right)^2 \right) - S \frac{\partial f}{\partial \zeta} - S \frac{\partial^2 f}{\partial \zeta^2} \frac{\zeta}{2} - M \sin^2 \gamma \frac{\partial f}{\partial \zeta} = 0, \quad (7)$$

$$\frac{\partial^2 \theta}{\partial \zeta^2} + \text{Pr} \lambda \left( 2 \frac{\partial f}{\partial \zeta} \theta - f \frac{\partial \theta}{\partial \zeta} + \frac{3}{2} S \theta + \frac{1}{2} S \zeta \frac{\partial \theta}{\partial \zeta} \right) + Nb \frac{\partial \theta}{\partial \zeta} \frac{\partial \chi}{\partial \zeta} + Nt \left( \frac{\partial \theta}{\partial \zeta} \right)^2 = 0, \quad (8)$$

$$\frac{\partial^2 \chi}{\partial \zeta^2} + Sc \lambda \left( \frac{3}{2} S \chi + \frac{\partial \chi}{\partial \zeta} f + \frac{1}{2} S \zeta \frac{\partial \chi}{\partial \zeta} - 2 \frac{\partial f}{\partial \zeta} \chi \right) + \frac{Nt}{Nb} \frac{\partial^2 \theta}{\partial \zeta^2} = 0, \quad (9)$$

with the transformed boundary conditions

$$\begin{aligned} f = 0, \frac{\partial f}{\partial \zeta} = 1, \theta = 1, Nb \frac{\partial \chi}{\partial \zeta} + Nt \frac{\partial \theta}{\partial \zeta} = 0, \text{ at } \zeta = 0, \\ f = \frac{\lambda}{2}, \frac{\partial \theta}{\partial \zeta} = \frac{\partial \chi}{\partial \zeta} = 0, \text{ at } \zeta = 1, \end{aligned} \quad (10)$$

where Pr represents the Prandtl number, S represents unsteadiness parameter,  $\lambda$  denotes the dimensionless film thickness,  $M$  represents magnetic field parameter,  $\gamma$  indicates aligned angle,  $Sc$  indicates the Schmidt number,  $Nb, Nt$  represents the Brownian motion, thermophoresis parameters respectively.

$$\left. \begin{aligned} \text{Pr} &= \frac{(\mu c_p)}{k}, M = \frac{\sigma B_0^2}{b\rho}, S = \frac{\alpha}{b}, \lambda = \beta^2, \alpha_m = \frac{k}{(\rho c_p)}, \\ \text{Sc} &= \frac{\nu}{D_B}, \text{Nt} = \frac{(\rho c_p)_s D_T (T_s - T_0)}{\alpha_m (\rho c_p)_f T_0}, \text{Nb} = \frac{(\rho c_p)_s D_B (C_s - C_0)}{(\rho c_p)_f \nu_f} \end{aligned} \right\} \quad (11)$$

For engineering interest, the local Nusselt number  $Nu_x$  is given by

$$\text{Re}_x^{-0.5} Nu_x = -\frac{1}{\beta} \theta'(0), \quad (12)$$

where  $\text{Re}_x = \frac{u_w x}{\nu_f}$  is the local Reynolds number.

### 3. Results and Discussion

The equations (7) to (9) with the conditions equation (10) are solved by employing shooting technique. For the numerical computation, we consider the emerging parameters as  $M = Le = 1, Nb = Nt = S = 0.5, \lambda = 0.3, \gamma = \pi/6$ . Figures 2-4 show the variation in flow, thermal and concentration fields for various values of the magnetic field parameter for Newtonian and non-Newtonian fluid flow cases. It is clear that the increasing values of the magnetic field parameter suppresses the flow field and encourages the thermal and concentration fields in both cases. This may be due to the drag force caused by the external magnetic field. It is also evident to mention that the Newtonian fluid is highly influenced by the external magnetic field when equated with the non-Newtonian fluid. The similar results has been observed for rising values of the aligned angle parameter as depicted in figures 5-7. Physically, rising values of the aligned angle strengthen the external magnetic field.

Figures 8-10 display the effect of unsteadiness parameter on velocity, temperature and concentration fields of both Newtonian and non-Newtonian fluid flow cases. It is evident that the increasing values of unsteadiness parameter declines the flow and thermal fields and enhances the concentration field of the both fluids. Generally, unsteadiness causes to oppose the buoyancy forces acts opposite to the flow field. The similar results are noticed for increasing values of the film thickness parameter (see figures 11-13).

Figures 14 and 15 illustrate the impact of thermophoresis parameter on thermal and concentration fields. We noticed that the increasing thermophoresis parameter enhance the thermal and mass concentration fields of both fluids. Physically, the moments of individual particles are different for different types of fluids. We noticed a decrease in concentration field for rising values of the Brownian motion and Schmidt number, which is depicted in figures 16 and 17. Generally, the random motion of the particles leads to decline the concentration field and hence enhance the mass transfer rate.

Table 1 shows the variations in the local Nusselt number for various values of the pertinent parameters. It is evident that the rising values of the aligned angle, transverse magnetic field and thermophoresis parameter decline the heat transfer rate. The opposite trend has been observed for increasing film thickness and unsteadiness parameters. The validation of the present results with various numerical techniques is depicted in Table2. We observed a reasonable agreement with the present technique.

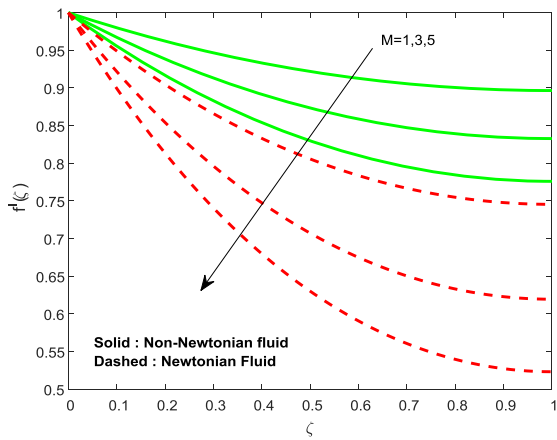


**Figure2.** Variation in the velocity field

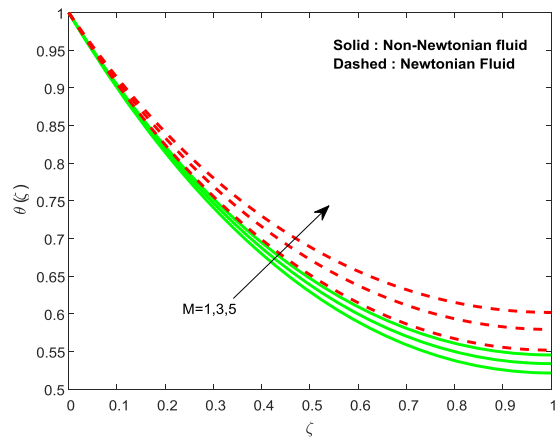


**Figure3.** Variation in the temperature field

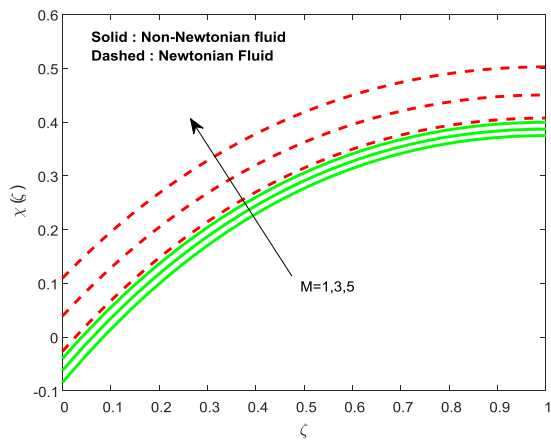


**Figure4.** Variation in the concentration field

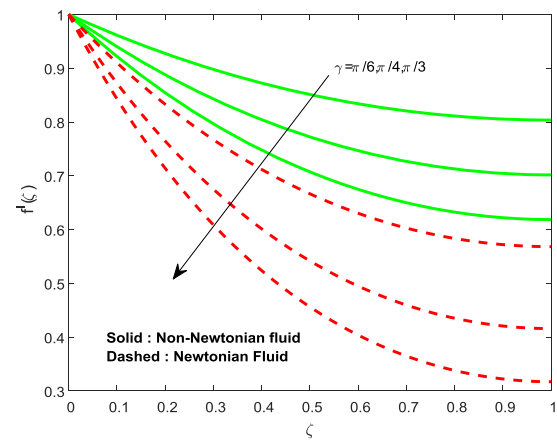


**Figure5.** Variation in the velocity field

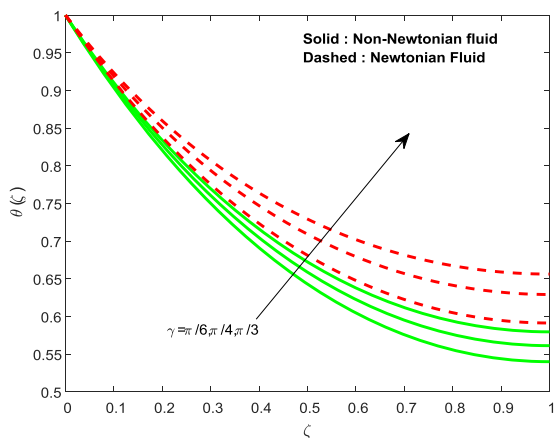


**Figure6.** Variation in the temperature field

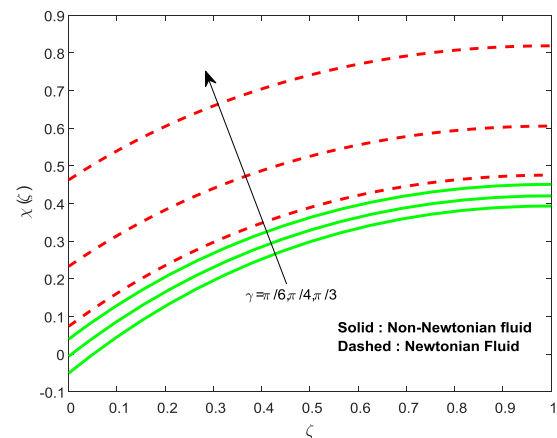


**Figure7.** Variation in the concentration field

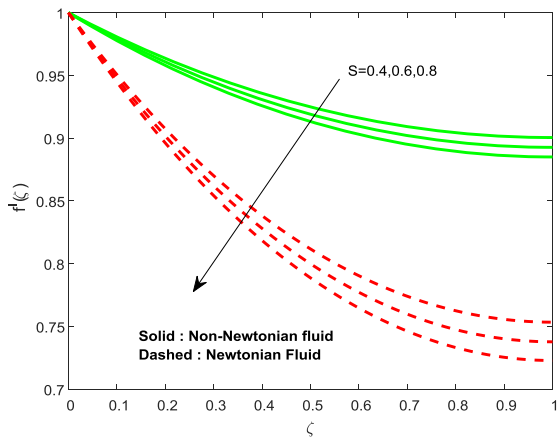


**Figure8.** Variation in the flow field

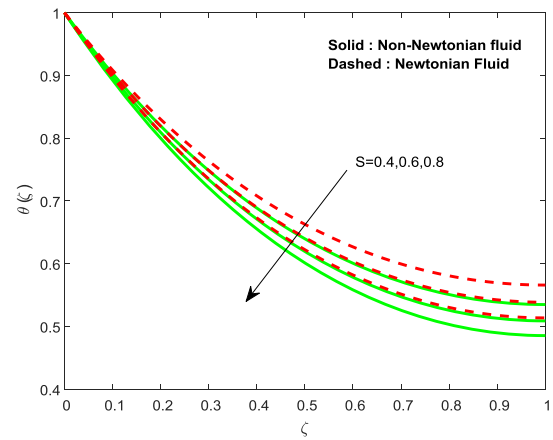


**Figure9.** Variation in the temperature field

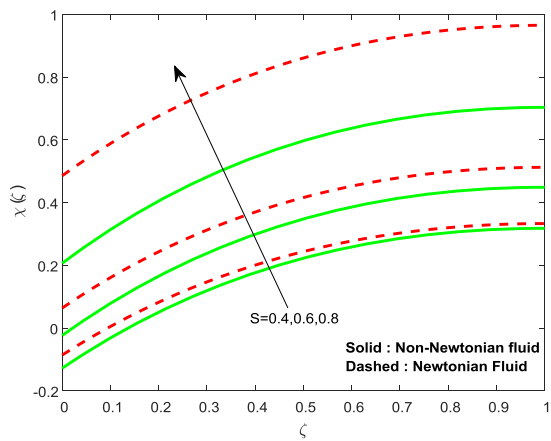


**Figure10.** Variation in the concentration field

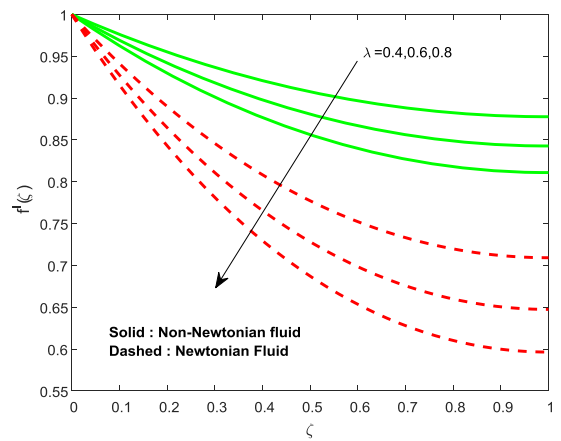


**Figure11.** Variation in the flow field

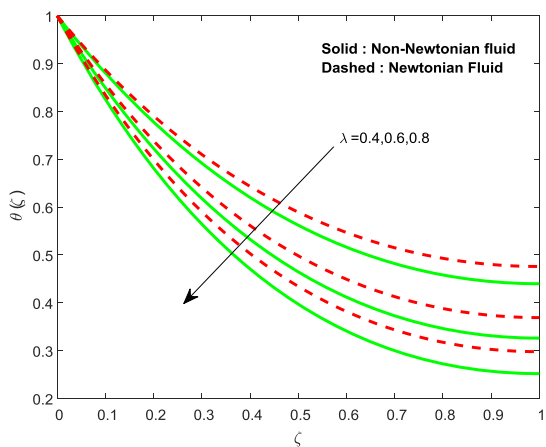


**Figure12.** Variation in the thermal field

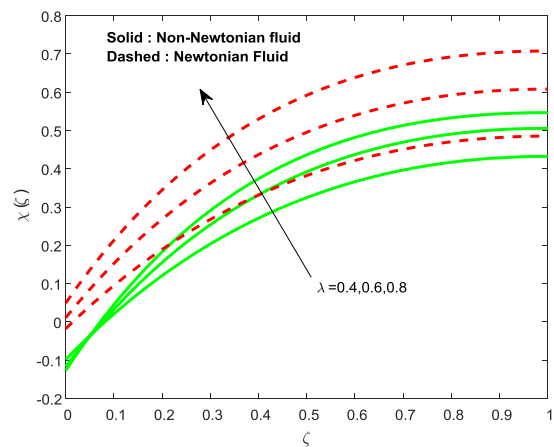


**Figure13.** Variation in the concentration field



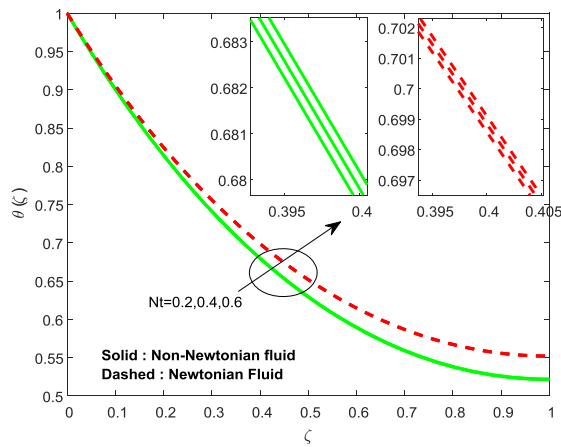


**Figure14.** Variation in the thermal field

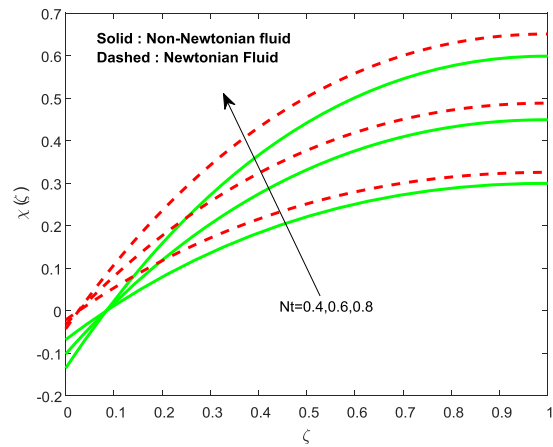


**Figure15.** Variation in the concentration field

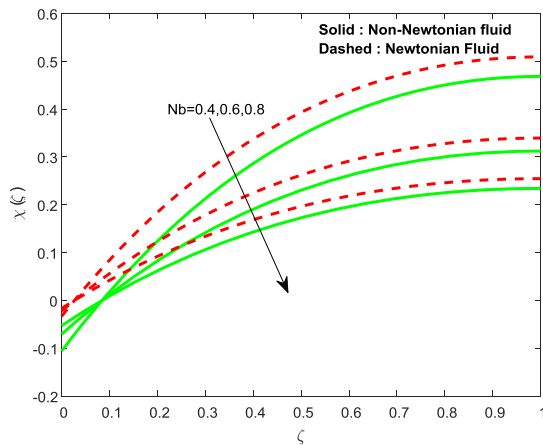


**Figure16.** Variation in the concentration field

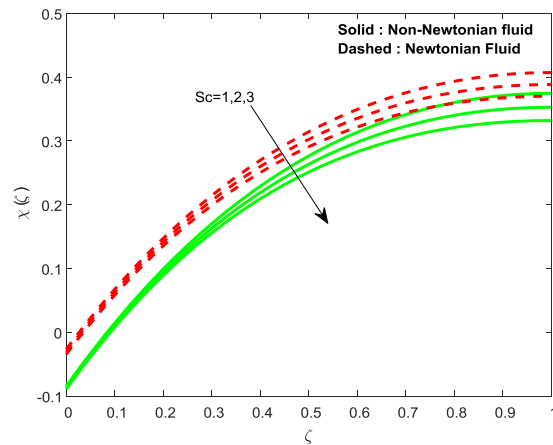


**Figure17.** Variation in the concentration field

**Table 1.** Variations in  $-\theta'(0)$  for Newtonian and non-Newtonian flow cases

$M$	$\gamma$	$S$	$\lambda$	$Nt$	Newtonian	Non-Newtonian
1					1.070136	1.017584
3					1.048575	0.970338
5					1.028744	0.931567
	$\pi/6$				1.038456	0.950037
	$\pi/4$				1.001807	0.885034
	$\pi/3$				0.970309	0.838196
		0.4			1.038712	0.984901
		0.6			1.100039	1.048788
		0.8			1.155826	1.107613
			0.4		1.292615	1.228326
			0.6		1.645654	1.564353
			0.8		1.921800	1.829305
				0.4	1.070759	1.018026
				0.6	1.069514	1.017142
				0.8	1.068273	1.016260



**Table 2.** Validation of the results of  $-\theta'(0)$  for several values of M for Newtonian fluid

$M$	$RKS$ (Present)	$BVP4C$	$BVP5C$	$RKF$
1	1.070136	1.0701363241	1.0701363242	1.0701363242
3	1.048575	1.0485755410	1.0485755410	1.0485755410
5	1.028744	1.0287447326	1.0287447325	1.0287447326

#### 4. Conclusion

We investigated the thermal and concentration transfer in unsteady liquid film flow of Casson fluid with effects of aligned magnetic field, thermophoresis and Brownian moment. The transformed governing boundary layer flow equations are analysed numerically by employing shooting technique. Dual solutions are explored for Newtonian and non-Newtonian cases. The impact of pertinent parameters on the flow, thermal and mass concentration fields are discussed with the assistance of graphical illustrations. Numerical observations of the present study are given below

- Heat and mass transfer rate is not uniform in Newtonian and non-Newtonian fluids.
- The impact of Lorentz force is high on non-Newtonian fluid.
- Unsteadiness causes to develop the reduced Nusselt number.
- Thermophoresis and Brownian motion regulates the thermal and concentration fields.
- Aligned magnetic field helps to control the flow field.

#### References

- [1] Sulochana C and Sandeep N 2016 *Appl Nanosci.* **6** 451-9
- [2] Sandeep N and Ganeswara Reddy M 2017 *J. Mol. Liq.* **225** 87-94
- [3] Crane L 1970 *ZAMP* **21** 645-7
- [4] Pop I and Na T 1998 *J Fluid Eng.* **25** 263-9
- [5] Liu I 2005 *Int Commun Heat Mass Transf* 321075-84
- [6] Chiam T 1995 *Int. J. Eng. Sci* **33** 429-35
- [7] Cortell R 2005 *Appl. Math. Comput.* **168** 557-66
- [8] Yi-wu Y 1985 *Appl Math Mech (English Edition)* **6** 259-68
- [9] Anjali DS and Thiyagarajan M 2006 *Heat Mass Transf* **42** 671-7
- [10] Pal D and Mondal H 2010 *Commun Nonlinear Sci Numer Simul* **15** 1197-209
- [11] Ishak A 2011 *Sains Malays* **40** 391–395
- [12] Nadeem S, Hussain ST and Changhoon Lee 2013 *Braz. J. Chem. Eng.* **30**(3) 619-25
- [13] Iffat Zehra, Malik Muhammad Yousaf and Sohail Nadeem 2015 *Results in Physics* **5** 20-5
- [14] Vajravelu K, Sreenadh S, Hemadri Reddy R and Murugesan K 2009 *Int J Mech Res* **36**(3) 244-54
- [15] Vajravelu K, Sreenadh S and Saravana 2013 *Appl. Math. Comput.* **225** 656-76
- [16] Sandeep N 2017 *Adv. Powder Technol.* **28** 865-5
- [17] Kumaran G and Sandeep N 2017 *J. Mol. Liq.* **233** 262-9
- [18] Saravana R, Sreekanth S, Sreenadh S and Hemadri Reddy R 2011 *Adv. Appl. Sci. Res.* **2**(1) 221-9
- [19] Reddy RH, Kavitha A, Sreenadh S and Saravana R 2011 *IJMME* **6**(2) 240-9
- [20] Hari Prabakaran P, Hemadri Reddy R, Saravana R, Kavitha A and Sreenadh S 2015 *AAFM* **17**(1) 1-16
- [21] Arun kumar M, Sreenadh S, Saravana R and Hemadri Reddy R 2016 *MJMS* **10**(1) 35-47
- [22] Saravana R, Sreenadh S, Venkataramana S, Hemadri Reddy R and Kavitha A 2011 *IJICTE* **1**(11) 10-24